Imaging of dielectric cylinders from experimental stepped-frequency data

Anthony Dubois, Jean-Michel Geffrin, and Kamal Belkebir[a)]
Institut Fresnel, UMR-CNRS 6133, Campus de Saint Jérôme, case 162, Université d'Aix-Marseille I and III, 13397 Marseille Cedex, France

Marc Saillard
LSEET, UMR-CNRS 6017, Université du Sud Toulon-Var, Boîte Postale 132, 83957 La Garde Cedex, France

(Received 24 November 2005; accepted 22 March 2006; published online 20 April 2006)

This letter reports on the characterization of two-dimensional targets from measured transient scattered fields. The problem is formulated in the frequency domain rather than directly in the time domain, and an iterative construction of the unknown dielectric constant is derived. Improvement of the resolution is suggested by marching on in the central frequency of the incident pulse. The efficiency of this approach is emphasized through examples of reconstructions of an inhomogeneous target from experimental data. © *2006 American Institute of Physics*. [DOI: 10.1063/1.2196067]

The realm of electromagnetic inverse scattering problems is to determine properties (geometry and/or constitutive material) of unknown objects from the measurement of their response (scattered field) to a known excitation (incident field). The most popular strategy is to iteratively build up the parameter of interest (relative permittivity profile) by minimizing a cost functional involving the discrepancy between the measurements and those that would be obtained via a scattering model with the best available estimation of the parameter. An accurate image of the object can be obtained from data recorded for a large number of angles under which the target under test is illuminated. However, the quality of the image deteriorates when reducing the aperture of illuminations. In the present letter, we consider only a single electromagnetic source that radiates a transient field; thus only a single illumination view of the target under test is used.

The resolution is restored by using a wide-band incident field. In Ref. 1, the authors show, using experimental data, that the distorted-wave Born iterative method provides a better image than the one obtained by processing the data under the Born approximation. It is interpreted, therein, as due to multiple scattering within the object under test. In practice, multiple scattering effects are taken into account in the inversion scheme by determining at each iteration step the internal field of the reconstructed object. In the present work, we follow the authors of Ref. 1 and show that unfortunately when the central frequency of the incident field is high, the inversion algorithm might be trapped into local minima,[2] unless an accurate initial guess is provided. A theoretical analysis of the dynamic range and the resolution of iterative inverse scattering algorithms has led to the idea of using as an initial guess the final result of the inversion at a lower frequency.[3] This is known as the frequency-hopping approach[4] and it has been successfully applied to experimental data.[5] In the case of stepped-frequency data measured on a large spectrum support (with a small frequency step), it is possible to synthesize pulses with different central frequencies, allowing one to apply a similar approach to the frequency-hopping technique. We describe below the experimental setup as well as the inversion algorithm used to process the data in order to illustrate the aforementioned ideas. All experiments were carried out in an anechoic chamber of dimensions of $14\times6.5\times6.5$ m^3. Many locations of the transmitting and receiving antennas could be used to measure the fields almost all around on a 4 m diameter sphere [Fig. 1(a)]. In the present study, we will only use the arrangement depicted in Fig. 1(b). The receiver remains in the azimuthal plane (xoy) and, for practical reasons, its excursion is restricted to the angle range of $60° \leqslant \theta \leqslant 300°$. Furthermore, as we are using a multifrequency approach, we have chosen to keep the source fixed, using thus a single incidence. The distance from the transmitter or receiver to the center of the target is 1.75 m and all the objects are long enough (1.5 m) to allow a two-dimensional (2D) assumption. The measurements were acquired with a vector network analyzer (VNA) (Agilent-HP 8510) used in a multisource setup with two synthesizers and two deported mixers. The transmitting and receiving antennas are both wide-band ridged horn antennas (ARA DRG118) and each measurement is performed with 300 evenly distributed frequencies from 1 up to 7 GHz. The electrical field is vertically polarized (along the z axis) in the azimuthal plane (xOy). The scattered field is extracted by subtracting the incident field (the field measured without any target) from the total field (the field in the presence of the target) and the receiver is moved from 60° to 300° with the angular step of 1°. The chosen scatterer [Fig. 2(c)] consists of dielectric cylinders with circular cross sections (one inside

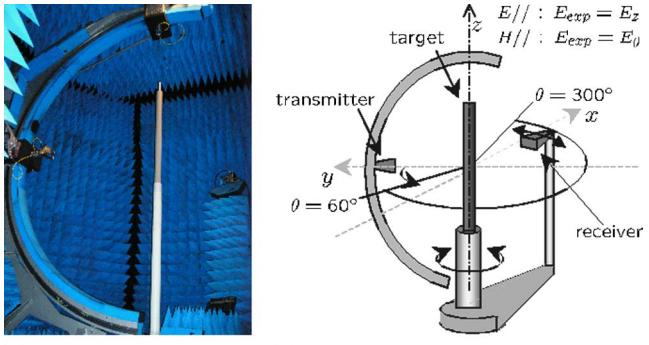

FIG. 1. (a) (Color online) Spherical measurement facility. (b) Source-receiver-object arrangement.

[a)]Electronic mail: kamal.belkebir@fresnel.fr

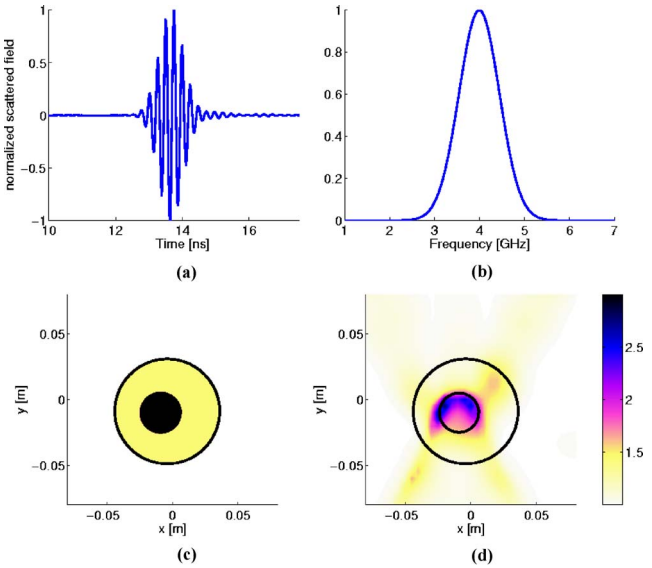

FIG. 2. (a) (Color online) Transient scattered field measured on the receiver at the front of the source. (b) Spectrum of the incident field. (c) Actual profile to be retrieved. (d) Result obtained with time domain data using the backpropagation method to obtain an initial guess. $f_0=4.0$ GHz and $\tau=2$ ns.

the other), the larger one of foam (SBF300) and 80 mm diameter and the smaller one of plastic (berylon) and 31 mm diameter. The dielectric constants of these plastics were measured with the commercial kit EpsiMu and were found to be almost constant in the 1–7 GHz band. The measured values of the relative permittivity were $\varepsilon_r=1.45$ and $\varepsilon_r=3$ for foam and for berylon, respectively. Furthermore, both materials present pratically no losses. The transient scattered field used as a datum for imaging the target under test is synthesized by weighting the time harmonic measured scattered fields by the spectrum of a chosen pulse shape and by carrying out the inverse temporal Fourier transform.

The inverse scattering problem is stated in the frequency domain, where for each frequency $l=1,\ldots,L$, the scattering problem may be formulated as two coupled contrast-source integral equations involving the total electric field E_l and the contrast distribution $\chi_l(\mathbf{r})=\varepsilon_{r,l}(\mathbf{r})-1$ ($\varepsilon_{r,l}$ being the complex relative permittivity). For the sake of simplicity, symbolic operator notations are used.

$$E_l^d = \mathbf{G}_{l,\Gamma}\chi_l E_l, \tag{1}$$

$$E_l = E_l^{\text{inc}} + \mathbf{G}_{l,\Omega}\chi_l E_l, \tag{2}$$

where E, E^{inc}, and E^d denote the total, incident, and scattered fields, respectively. $\mathbf{G}_{U=\Omega,\Gamma}$ represents an integral operator whose kernel involves the two-dimensional free space Green function. The aim is to determine the permittivity distribution in a bounded box Ω, such that the corresponding scattered field matches the measured one. An iterative approach is used to solve this ill-posed and nonlinear problem.[6] In this approach, starting from an initial guess, the parameter of interest (the permittivity distribution) is gradually adjusted by minimization of a cost function $\mathcal{F}$ of the form

$$\mathcal{F}(E_l;\chi) = \frac{\sum_{l=1}^{L}\|h_l^{(1)}\|_\Omega^2}{\sum_{l=1}^{L}\|E^{\text{inc}}\|_\Omega^2} + \frac{\sum_{l=1}^{L}\|h_l^{(2)}\|_\Gamma^2}{\sum_{l=1}^{L}\|f_l\|_\Gamma^2}, \tag{3}$$

where the residual errors $h^{(1)}$ and $h^{(2)}$ are defined as follows:

$$h_l^{(1)} = E_l^{\text{inc}} - E_l + \mathbf{G}_{l,\Omega}\chi_l E_l, \tag{4}$$

$$h_l^{(2)} = f_l - \mathbf{G}_{l,\Gamma}\chi_l E_l. \tag{5}$$

By virtue of the Parseval theorem, minimizing the cost function described in Eq. (3) in the frequency domain is equivalent to minimizing the same cost function in the time domain where the time-harmonic field quantities are replaced by the corresponding transient ones and where the sum is over time instead of over frequency. To improve the efficiency of the algorithm, we add *a priori* information stating that the desired electrical susceptibility must be greater than unity and the conductivity positive. With these conditions and assuming an Ohmic dispersion model for materials of interest, the contrast function χ_l reads as

$$\chi_l = 1 + \xi_n^2 - \frac{i\eta_n^2}{\omega_l\varepsilon_0} - \varepsilon_{rb}. \tag{6}$$

In the inversion method described here, ξ_n, η_n (real), and $E_{l,n}$ (complex) associated with the permittivity, the conductivity, and the total field in Ω, respectively, are computed at each iteration step, according to the following relations:

$$E_{l,n} = E_{l,n-1} + \alpha_{l,n;v}v_{l,n} + \alpha_{l,n;w}w_{l,n}, \tag{7}$$

$$\xi_n = \xi_{n-1} + \beta_{n;\xi}d_{n;\xi} \quad \text{and} \quad \eta_n = \eta_{n-1} + \beta_{n;\eta}d_{n;\eta}. \tag{8}$$

In the three recursive relations in (7) and (8), $v_{l,n}$, $d_{n,\xi}$, and $d_{n,\eta}$ are updating directions given by the standard Polak-Ribière conjugate gradient method, and $w_{l,n}$ is another updating direction defined as

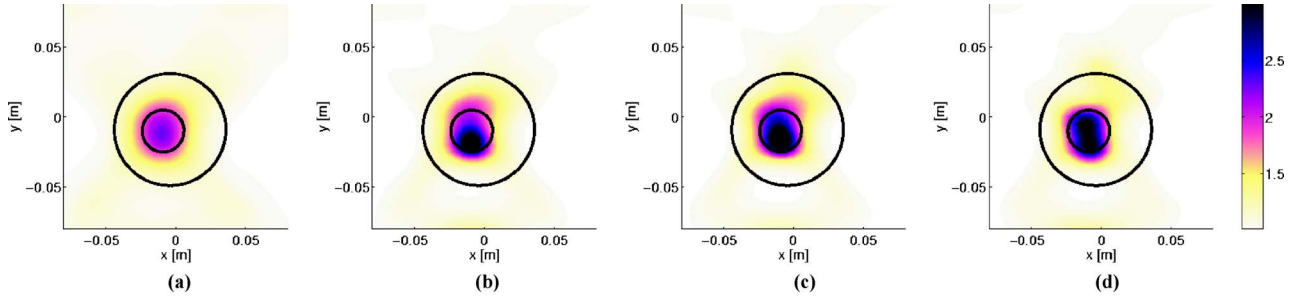

FIG. 3. (Color online) Map of the reconstructed permittivity using the central-frequency-hopping approach. (a) Result with $f_0=2.5$ GHz using the backpropagation method to obtain the initial guess. (b) Result with $f_0=3.0$ GHz with (a) as initial guess. (c) Result with $f_0=3.5$ GHz with (b) as initial guess. (d) Result with $f_0=4.0$ GHz with (c) as initial guess.

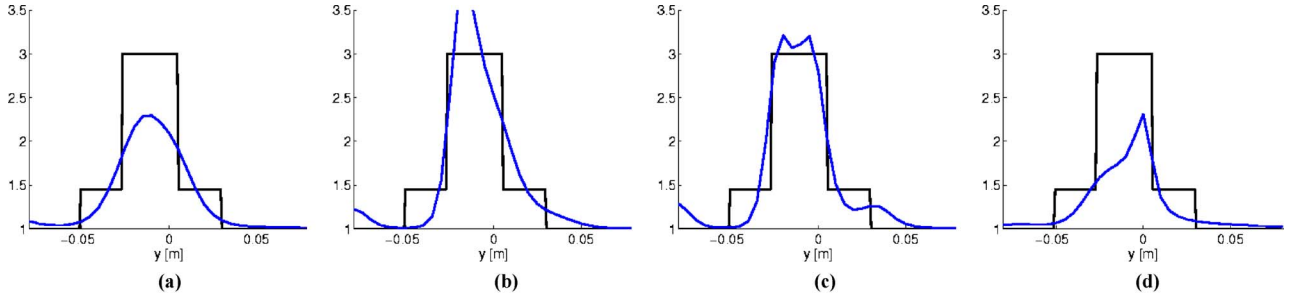

FIG. 4. (Color online) Comparison between the reconstructed permittivity profile (blue line) and the actual one (black curve) along the direction of the illumination Oy. (a), (b), (c), and (d) correspond to reconstructions presented in Figs. 3(a), 3(c), 3(d), and 2(d), respectively.

$$w_{l,n} = \widetilde{E}_{l,n-1} - E_{l,n-1}, \quad \widetilde{E}_{l,n-1} = [1 - \mathbf{G}_{l,\Omega}\chi_{n-1}]^{-1} E_l^{\text{inc}}. \quad (9)$$

The field $\widetilde{E}_{l,n}$ corresponds to the total field computed from field equation (2) with the contrast χ_{n-1}. In practice, the computation of $\widetilde{E}_{l,n-1}$ uses a fast forward solver. Details of this forward solver are given in Ref. 7. The two complex coefficients $\alpha_{l,n;v}$ and $\alpha_{l,n;w}$ and the real coefficients $\beta_{n;\xi}$ and $\beta_{n;\eta}$ are determined at each iteration step by minimizing the cost function $\mathcal{F}_n$ defined in Eq. (3).

In this section we report the reconstruction of the inhomogeneous dielectric target [Fig. 2(c)] from transient scattered fields using the inversion algorithm presented in the previous section. In all cases the investigated domain Ω was a large 16 cm square domain and discretized for numerical purposes into 33×33 square cells. All the reported final results correspond to the 20th iteration. We did not note any marked changes in the results when continuing iterating. In addition, only the real part of the reconstructed permittivity is presented since the imaginary part remains very small in all cases. Measurements of the scattered field were carried out over 300 frequencies, evenly distributed on the 1–7 GHz frequency band. The transient scattered field is determined by performing the temporal Fourier transform, thus making possible to choose different incident pulse shapes. We start with a Gaussian incident pulse shape $F(t)$ whose spectrum is centered at $f_0 = 4$ GHz and of time duration $\tau = 2$ ns,

$$F(t) \propto \exp\left[-16\frac{(t-\tau)^2}{\tau^2}\right]\sin(2\pi f_0 t). \quad (10)$$

The measured transient scattered field on the receiver in front of the source located at (0 m; 1.75 *m*) and the corresponding spectrum of the incident pulse are reported in Figs. 2(a) and 2(b), respectively. Figure 2(d) presents the result of the inversion with the initial guess deduced from a backpropagation procedure.[8] The target is clearly not characterized. Indeed we obtained information only on a part of the contour of the smallest dielectric cylinder. The inversion algorithm is in this case trapped into a local minimum of the minimized cost function.[2] To avoid this local minimum, we investigate a better initial guess than the one provided by a backpropagation procedure. To this end, a central-frequency-hopping approach is applied, i.e., the initial guess for the inversion is given by the final result obtained using a pulse with a lower central frequency. This is equivalent to successively illuminating targets with different incident fields having spectra centered at increasing frequencies. Results of this approach are reported in Fig. 3 where one can clearly notice the gradual improvement of the resolution. Figure 3(a) corresponds to the inversion with $f_0 = 2.5$ GHz, the initial guess being the one deduced by the backpropagation procedure. Figures 3(b)–3(d) present reconstructions using pulses with $f_0 = 3$, 3.5, and 4 GHz, respectively, and where the initial guesses are now the final results with pulses of lower central frequencies. To emphasize the improvement of the resolution, quantitative comparisons of the reconstructed profiles along the direction of the illumination are given in Fig. 4. Notice that all pulses are of the same time duration $\tau = 2$ ns and Figs. 3(d) and 4(c) are to be compared with Figs. 2(d) and 4(d), respectively, since the same transient data were used. Targets can now be characterized, and we obtained information not only on the face in front of the source but also on the "hidden" face. In this letter, we discussed the problem of the characterization of targets using a transient scattered field. To improve the resolution, we proposed a method based on the frequency-hopping technique. This approach was successfully tested against experiment. We noticed a significant improvement of the resolution of the final result using the central frequency hopping in comparison with the one obtained without using the proposed method.

[1] Fu-C. Chen and W. C. Chew, Appl. Phys. Lett. **72**, 3080 (1998).
[2] O. M. Bucci, L. Crocco, T. Isernia, and V. Pascazio, IEEE Trans. Geosci. Remote Sens. **GE-38**, 1316 (2000).
[3] A. G. Tijhuis, K. Belkebir, A. C. S. Litman, and B. P. de Hon, IEEE Trans. Geosci. Remote Sens. **GE-39**, 1316 (2001).
[4] W. C. Chew and J. H. Lin, IEEE Microw. Guid. Wave Lett. **15**, 439 (1995).
[5] A. G. Tijhuis, K. Belkebir, A. C. S. Litman, and B. P. de Hon, Inverse Probl. **17**, 1635 (2001).
[6] K. Belkebir and A. G. Tijhuis, Inverse Probl. **17**, 1671 (2001).
[7] Z. Q. Peng and A. G. Tijhuis, J. Electromagn. Waves Appl. **7**, 739 (1993).
[8] R. E. Kleinman and P. M. van den Berg, Radio Sci. **29**, 1157 (1994).